

Direct Evidence for a Coordination-Insertion Mechanism in Ethylene Oligomerization Catalysed by Neutral 2,6-Bisiminopyridine Iron Monoalkyl Complexes.

M. Ángeles Cartes, Antonio Rodríguez-Delgado, Pilar Palma, Luis J. Sánchez and Juan Cámpora.*

Supplementary Information

- 1. Experimental Procedures**
- 2. Preliminary DFT Calculations**
- 3. References**
- 4. Atomic Coordinates (B3LYP/6-31+G*) and Energies (M06/6-31++G**//B3LYP/6-31+G*) for the model molecules Ethylene, 2', 3'-d and 3'-q.**

1. Experimental Procedures

General: All manipulations were carried out under oxygen-free argon atmosphere using conventional Schlenck techniques, or a nitrogen filled glove box. Solvents and mesitylene were rigorously dried and degassed before using. Compounds **1** and **2** were prepared according to literature procedures.^{1,2} NMR spectra were recorded on Bruker DRX 300 or 400 spectrometers. The residual resonance of the solvent were used as the internal standard but chemical shifts were reported with respect to TMS. GC analysis were run in an Agilent model 6890 chromatograph equipped with a Tchnochroma TRB1 column and a TCD detector.

Monitoring the reaction of compounds 1 and 2 with ethylene at the room temperature: In the glove box, stock solutions containing the specified concentration of the complex (11 or 20 mM) and a 10 % mol amount of mesitylene (as internal standard) in C₆D₆ were prepared. NMR tubes were charged with 0.7 ml of these solutions (i. e., 8 or 14 μmol of the corresponding Fe complex, respectively) and capped with a septum, taken out of the glove-box and the prescribed volume of ethylene was injected through the septum using a gas-tight syringe fitted with a narrow (0.6 mm), long needle. The septum was then sealed with a bit of silicone grease and Parafilm®. Gas consumption was ¹H NMR monitored using the more diluted catalyst solutions (11 mM). In order to detect intermediate species, four tubes containing samples of the more concentrated solution (20 mM) were treated with different volumes of ethylene (1, 2, 5 or 10 ml) and NMR spectra were taken at different times. Signals of the intermediates formed from complex **2** were best observed in the sample treated with 5 ml of ethylene. Their intensity was not significantly increased in the 10 ml ethylene sample probably because the solvent is already saturated with ethylene, but the quality of the spectrum was somewhat poorer. In order to gather the temporal sequence shown in Figure 2, the 5 ml experiment was repeated and ¹H NMR spectra recorded at the indicated reaction times.

The diamagnetic region of the ¹H NMR spectra provided information on the oligomerization process (Figure S1). Spectra taken after 5 min showed that ethylene had been consumed and showed two signals with 1:2 intensity ratio at δ 5.27 and 4.39 ppm due to terminal vinyl groups. After the samples were allowed to stand at room temperature for 4.5 h, the NMR spectrum showed a new signal at 5.36 ppm due to the presence of internal olefins arising from the slower isomerization process. GC analysis required piercing the septum with a GC syringe, which is likely to allow the admission of some air, destroying part of the catalyst and thus preventing continuous reaction monitoring. Therefore, ethylene oligomerization and the subsequent olefin isomerization were detected in different experiments. Figure S2 shows two representative examples of GC analyses. On the left (A), there is an analysis of a sample oligomerized using complex **1**, after 10 min reaction time, which shows even number of carbon α-olefins

with a regular spacing corresponding to increases in two CH₂ units. The GC on the right corresponds to a sample obtained with compound **2**, after it was allowed to stand overnight. As can be seen, each cluster of signals contains essentially three components. Comparison of the retention times with those of commercial samples of 1-octene and trans-2-octene shows that the two first peaks in each cluster of signals correspond to the α -olefin and trans-2-olefin, and therefore the closely following third signal likely corresponds to the cis-2-olefin.

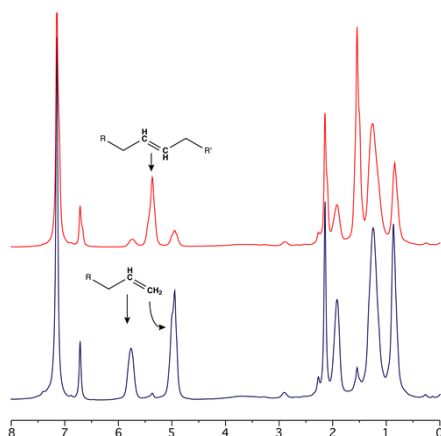


Figure S1. ¹H NMR monitoring of ethylene oligomerization with complex **2**, showing the signals of oligomers. Down (blue), after 10 min, terminal vinyl groups. Up (red), after 4.5 h, showing partial isomerization of α -olefins into internal olefins.

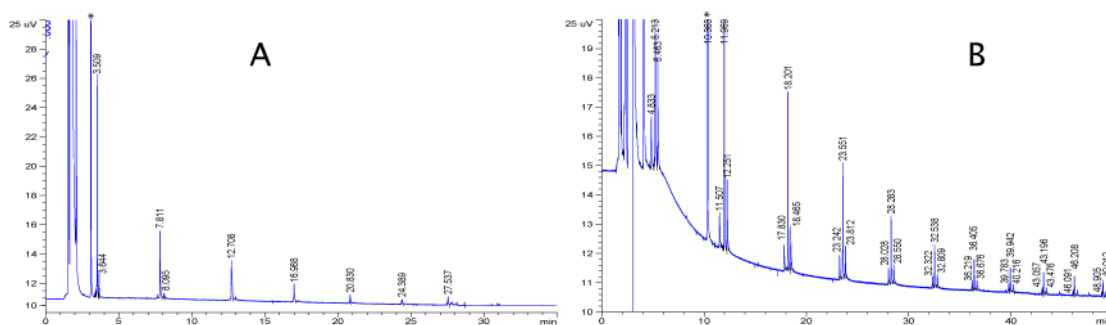


Figure S2. Two representative GC traces corresponding to two different experiments, showing the distribution of ethylene oligomers. **A**, with complex **1**, 10 min reaction time; **B**, allowing the reaction mixture to stand for an extended period of time (complex **2**). Peaks marked with asterisk correspond to mesitylene.

Variable temperature experiments: A solution containing 5.5 mg (10 μ mol) of compound **2** in toluene-*d*₈ was prepared in the glove box and transferred into an NMR sample tube capped with a rubber septum. The sample was taken from the glove box and placed in a cooling bath at -20° C. Ethylene (0.6 ml) was

smoothly injected into the sample using a gas-tight syringe fitted with a narrow needle (0.6 mm). The septum was sealed with a bit of silicone grease and Parafilm®. The sample was then transferred to the precooled (-50 °C) NMR probe.

2. Preliminary DFT calculations.

Preliminary DFT calculations have been carried out in order to determine the energy change associated to the interaction of Fe monoalkyl compounds with ethylene. To this purpose, the isopropyl groups of the ⁱPrBIP ligand were replaced with methyl groups. Guess structures were calculated using the Spartan14 program, and the final geometry and energies were calculated with Gaussian09. Geometries of the model complex and the corresponding ethylene adduct was determined at the B3LYP/6-31+G* level. Energies were refined with single point calculation using the M06 functional and 6-311++G** basis functions in all atoms. The B3LYP/6-31+G* model was selected because the optimized structure of the simplified methyl complex (**2'**) compares somewhat better with the experimental X-ray diffraction data for the related monoalkyls **2** and [Fe(CH₂SiMe₃)(^{mes}BIP)] than the structures obtained with other theoretical models (e. g. BP86 or B3LYP functionals with 6-31G* basis functions the light atoms and SDD pseudopotential on Fe), at a reasonable computational cost. The geometry of the methyl complex was optimized for a high-spin (S=4), configuration, as this has been found to be the most stable for this type of complexes.^{2,3} However, since the ethylene adduct was not previously studied, both high spin (S = 4, **3'-q**) and low spin (S=2, **3'-d**) were considered (Figure S3). In this case, the low spin configuration was found to be more favourable both at the B3LYP/6-31+G* level (ΔE (doublet-quartet) = -13.0 Kcal/mol) and M06/6-311++G** (-16.7 Kcal/mol) theory levels. The fact that, in contrast with monoalkyl **2**, the ¹H NMR spectrum of the ethylene complex **3** cannot be observed could be related to the S=2 electronic configuration favoured in the latter complex.

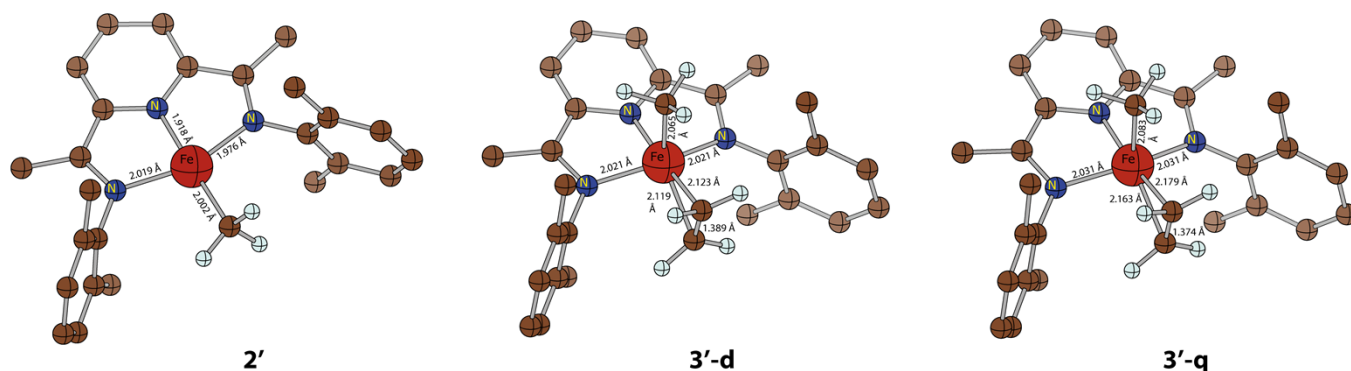
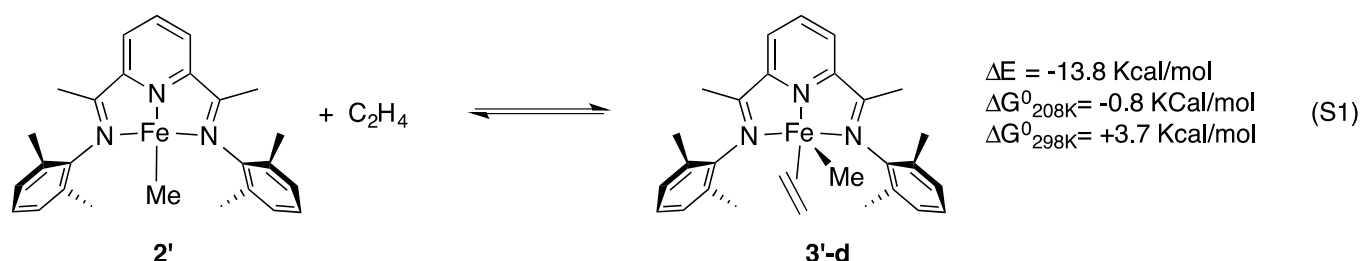


Figure S3. Optimized structures of model molecules **2'**, **3'-d** y **3'-q**, showing some key bond distances. Hydrogen atoms of the BIP ligands have been omitted for clarity.

In order to calculate the energy change associated to the formation of the formation of the ethylene adduct (Eq 1), the M06/6-311+G** was corrected with the free energy correction calculated at the B3LYP/6-31+G*, according to Eq. 2. As indicated in Eq 1, the favourable electronic energy change, -13.8 Kcal/mol, is offset by the entropic contribution, giving a positive variation of ΔG at room temperature (+3.7 Kcal/mol). At -65 °C, the entropic contribution is lower and the variation of free energy becomes negative, -0.8 Kcal/mol, very similar to the -1 Kcal/mol experimental estimate for **2/3**. Although the formation of complex **3'** would be expected to be more favourable than that of **3**, owing to the less hindered environment of the Fe atom, it should be considered that the gas phase calculation probably overestimates the entropy contribution in condensed phase.



$$\Delta G^0_{\text{T}}(\text{M06/6-311+G}^{**}) = \Delta E(\text{M06/6-311+G}^{**}) + \Delta G^0_{\text{T}}(\text{B3LYP/6-31+G}^*) - \Delta E(\text{B3LYP/6-31+G}^*) \quad \square \text{S} \square$$

□

3. References

□□□□ M. A. Cartes, A. Rodríguez-Delgado, P. Palma, E. Álvarez, J. Cámpora, *Organometallics*, 2014, **33**, 1834.

2) M. W. Bouwkamp, S. C. Bart, E. J. Hawrelak, R. J. Trovitch, E. Lobkovsky, P. J. Chirik, *Chem. Commun.*, 2006, 3406.

□□□ A. M. Tondreau, C. Milsman, A. D. Patrick, H. M. Hoyt, E. Lobkovsky, K. Wieghardt, Paul J. Chirik, *J. Am. Chem. Soc.* 2010, **132**, 15046.

4. Atomic Coordinates (B3LYP/6-31+G*) and Energies (M06/6-31++G//B3LYP/6-31+G*) for the model molecules Ethylene, 2', 3'-d and 3'-q.**

Ethylene: E = -78,53837741 Hartree

C	0.000000	0.000000	0.667420
H	0.000000	0.924157	1.241605
H	0.000000	-0.924157	1.241605
C	0.000000	0.000000	-0.667420
H	0.000000	-0.924157	-1.241605
H	0.000000	0.924157	-1.241605

Complex 2': E = -2436,131842 Hartree

H	0.017233	5.656680	0.006564
C	0.020037	4.570821	0.003782
N	0.017739	1.817723	-0.003829
C	-1.200653	3.871567	0.002782
C	1.236675	3.876465	0.002421
C	1.218594	2.476361	-0.000991
C	-1.188340	2.477490	-0.000584
H	-2.135493	4.422697	0.005306
H	2.173737	4.423659	0.004636
C	2.322949	1.550999	-0.000327
C	-2.306693	1.557554	-0.000009
Fe	0.012342	-0.100576	-0.007284
N	-1.973837	0.261140	-0.000687
N	1.953927	0.264489	-0.001398
C	0.063836	-2.101877	-0.009180
H	-0.924019	-2.581619	-0.018906
H	0.605649	-2.469663	0.878226
H	0.623303	-2.469451	-0.885495
C	-3.006377	-0.727952	0.000551
C	-4.976031	-2.709502	0.003438
C	-3.481180	-1.230406	1.229556
C	-3.485062	-1.230110	-1.227063
C	-4.476719	-2.219053	-1.203377
C	-4.472923	-2.219319	1.208788
H	-4.852537	-2.612226	-2.145666
H	-4.845782	-2.612697	2.152166
H	-5.743955	-3.478948	0.004555
C	2.974393	-0.743566	0.000679
C	4.921954	-2.742808	0.005046
C	3.450875	-1.245032	-1.227149
C	3.444665	-1.245723	1.230617
C	4.425250	-2.245758	1.209984
C	4.431348	-2.245084	-1.202109
H	4.795318	-2.641111	2.153521
H	4.806168	-2.639922	-2.143984

H	5.680599	-3.521354	0.006743
C	2.906373	-0.734516	-2.540669
H	3.065425	0.343780	-2.666978
H	1.824676	-0.902661	-2.612463
H	3.386281	-1.244508	-3.382271
C	-2.919471	-0.736767	-2.537546
H	-3.072287	0.340538	-2.680061
H	-3.386493	-1.255460	-3.381186
H	-1.836719	-0.909229	-2.585310
C	-2.911556	-0.737152	2.538325
H	-3.065709	0.339794	2.682213
H	-1.828358	-0.907687	2.581896
H	-3.374601	-1.257253	3.383288
C	2.893749	-0.735616	2.541622
H	3.053591	0.342380	2.669612
H	3.368482	-1.246897	3.385373
H	1.811465	-0.902279	2.607450
C	3.762256	1.990831	0.002371
H	3.845424	3.079882	0.002841
H	4.298044	1.610242	-0.875693
H	4.294887	1.609689	0.882127
C	-3.736800	2.025109	0.001694
H	-3.805830	3.114828	0.002324
H	-4.274669	1.648810	0.880472
H	-4.276413	1.649771	-0.876427

Complex 3'-d. E = -2514,692263 Hartree

H	0.000006	5.626129	-0.558383
C	0.000010	4.549687	-0.417913
N	0.000006	1.798264	-0.048847
C	-1.211572	3.850856	-0.337953
C	1.211580	3.850870	-0.337928
C	1.200238	2.465384	-0.163691
C	-1.200212	2.465383	-0.163715
H	-2.150942	4.387430	-0.424195
H	2.150951	4.387449	-0.424146
C	2.311903	1.558982	-0.131731
C	-2.311903	1.558973	-0.131769
Fe	0.000034	0.009895	0.431150
N	-1.953261	0.276510	-0.015239
N	1.953228	0.276500	-0.015209
C	-0.000065	0.605442	2.408316
H	-0.887478	1.235467	2.546488
H	0.887217	1.235643	2.546529
H	-0.000009	-0.187855	3.163388
C	-0.000005	-1.960920	1.220669

H	-0.915481	-2.117878	1.783812
H	0.915443	-2.117922	1.783847
C	0.000020	-2.022813	-0.166797
H	-0.918390	-2.233331	-0.706465
H	0.918437	-2.233388	-0.706432
C	3.743164	2.007706	-0.265395
H	3.818955	3.096325	-0.309839
H	4.205125	1.600012	-1.173309
H	4.351551	1.661863	0.578018
C	-3.743156	2.007725	-0.265451
H	-4.205072	1.600121	-1.173428
H	-3.818943	3.096348	-0.309788
H	-4.351578	1.661792	0.577898
C	2.979716	-0.720768	-0.120034
C	4.917976	-2.720323	-0.400191
C	3.665279	-1.186384	1.022360
C	3.270359	-1.237173	-1.403323
C	4.242561	-2.238506	-1.520950
C	4.629026	-2.191088	0.856862
H	4.466169	-2.643396	-2.505632
H	5.159892	-2.557586	1.732843
H	5.665825	-3.502161	-0.505815
C	-2.979744	-0.720756	-0.120064
C	-4.917957	-2.720360	-0.400160
C	-3.665322	-1.186321	1.022338
C	-3.270352	-1.237226	-1.403336
C	-4.242531	-2.238587	-1.520931
C	-4.629047	-2.191051	0.856872
H	-4.466113	-2.643531	-2.505596
H	-5.159931	-2.557504	1.732859
H	-5.665790	-3.502216	-0.505758
C	3.409461	-0.610639	2.396057
H	2.354729	-0.664963	2.675937
H	3.689293	0.449476	2.452660
H	3.995496	-1.146356	3.149909
C	2.559431	-0.716746	-2.631164
H	1.470874	-0.749484	-2.510327
H	2.831218	-1.305397	-3.513392
H	2.815904	0.330709	-2.837918
C	-3.409531	-0.610497	2.396008
H	-3.995896	-1.145904	3.149823
H	-3.688956	0.449731	2.452435
H	-2.354867	-0.665191	2.676088
C	-2.559403	-0.716859	-2.631191
H	-2.815823	0.330603	-2.837970
H	-2.831222	-1.305517	-3.513405
H	-1.470846	-0.749649	-2.510359

Complex **3'**-q. E = -2514,665576 Hartree

H	0.000198	5.648707	-0.638414
C	0.000155	4.570604	-0.494431
N	0.000037	1.846434	-0.083777
C	-1.218653	3.894073	-0.412521
C	1.218903	3.894005	-0.412306
C	1.190857	2.478263	-0.216495
C	-1.190719	2.478329	-0.216736
H	-2.161078	4.422441	-0.499464
H	2.161376	4.422310	-0.499113
C	2.294553	1.566023	-0.179048
C	-2.294471	1.566150	-0.179473
Fe	-0.000073	0.014815	0.389547
N	-1.966331	0.265478	-0.052369
N	1.966302	0.265372	-0.052099
C	-0.000247	0.723710	2.347970
H	-0.888798	1.355721	2.457284
H	0.887995	1.356149	2.457386
H	-0.000128	-0.040437	3.132344
C	-0.000220	-1.933883	1.365281
H	-0.920041	-1.989765	1.938928
H	0.919430	-1.989822	1.939206
C	-0.000042	-2.113051	0.003381
H	-0.923545	-2.326913	-0.526103
H	0.923603	-2.326992	-0.525831
C	3.701098	2.080502	-0.322469
H	3.953606	2.766886	0.497656
H	3.812181	2.649939	-1.255513
H	4.433118	1.270948	-0.329443
C	-3.700979	2.080717	-0.322947
H	-3.812153	2.649692	-1.256263
H	-3.953274	2.767550	0.496868
H	-4.433096	1.271245	-0.329375
C	2.982347	-0.736750	-0.118222
C	4.879491	-2.792778	-0.304316
C	3.700488	-1.130047	1.033121
C	3.231584	-1.352504	-1.367078
C	4.181340	-2.379425	-1.438898
C	4.640053	-2.164348	0.917150
H	4.372939	-2.856297	-2.397831
H	5.192487	-2.473999	1.801830
H	5.609417	-3.595432	-0.372764
C	-2.982551	-0.736512	-0.118382
C	-4.879464	-2.792784	-0.304217
C	-3.700722	-1.129711	1.033020
C	-3.231598	-1.352562	-1.367113
C	-4.181219	-2.379620	-1.438800

C	-4.640185	-2.164111	0.917154
H	-4.372574	-2.856805	-2.397626
H	-5.192646	-2.473674	1.801848
H	-5.609280	-3.595545	-0.372569
C	3.505726	-0.436870	2.361797
H	2.454843	-0.400300	2.660260
H	3.854612	0.603583	2.326622
H	4.071539	-0.947225	3.148113
C	2.505041	-0.896967	-2.611149
H	1.416577	-0.949952	-2.489871
H	2.785685	-1.512901	-3.471804
H	2.737145	0.147547	-2.854532
C	-3.505897	-0.436543	2.361683
H	-4.073294	-0.945717	3.147622
H	-3.852821	0.604534	2.325961
H	-2.455228	-0.401786	2.661092
C	-2.504565	-0.897609	-2.611114
H	-2.736638	0.146762	-2.855149
H	-2.784804	-1.514006	-3.471569
H	-1.416153	-0.950452	-2.489342